Interactions of Cumulus Convection and the Boundary Layer at the Southern Great Plains ACRF

Final Report

for the period May 15, 2008 to May 14, 2013

Steven K. Krueger
Principal Investigator

Department of Atmospheric Sciences
University of Utah
Salt Lake City, Utah USA 84112

September 2014

Prepared for

THE U.S. DEPARTMENT OF ENERGY
Grant DE-FG02-08ER64553

Contents

1 Executive Summary

The DOE ARM program has promoted understanding of cumulus convection by producing high-quality "single-column model" observational datasets that allow one to run and evaluate single-column models and cloud-resolving models based on observed large-scale conditions. The cloud and radiation fields produced by such simulations can then be compared to measurements by an ARM cloud profiling radar, as well as to satellite-based measurements. This is an excellent approach for stratiform cloud systems, but not for convective cloud systems, which are inadequately sampled by the cloud profiling radars. However, the existing observational systems at the ARM Southern Great Plains (SGP) Atmospheric Climate Research Facility (ACRF) can be used to provide a much more extensive spatial sampling of convective cloud systems. Because convective cloud systems generally have strong interactions with boundary layer circulations and thermodynamics, the boundary layer wind and thermodynamic fields contain a great deal of information about convective cloud systems and their interactions with the boundary layer.

We developed new methods to "retrieve" information about convective cloud systems from mesonet and precipitation data. Our data products are based on 15 years of 5-minute Oklahoma Mesonet data and hourly Arkansas Basin River Forecast Center (ABRFC) gridded precipitation data and include (1) statistics of the surface divergence field from which estimates of near-cloud-base updraft and downdraft mass fluxes can be made, and (2) catalogs of (a) frontal passage properties (time and location, temperature drop and pressure rise), and (b) convective cold pool properties (time and location, size, duration, temperature drop and pressure rise).

2 Comparison of Actual Accomplishments with Project Goals

2.1 Goals and objectives

Our research goals were to thoroughly investigate the following hypotheses:

1. Updraft and downdraft cumulus mass fluxes can be retrieved or estimated from surface mesonet observations of wind velocity combined with gridded precipitation rate.

2. Cold pool properties can be retrieved or estimated from surface mesonet observations of temperature, water vapor, and pressure.

3. Convective system evolution depends on cold pool development.

4. A prognostic cumulus parameterization that predicts both cloud-scale and mesoscale cumulus kinetic energy will exhibit improved convection initiation (triggering).

5. Cumulus parameterizations need to consider elevated convection initiation, not just surface-based.

We proposed to produce a number of datasets based on Oklahoma Mesonet data and gridded precipitation data for 13 warm seasons. Our proposed data products included the following hourly time series for the Oklahoma Mesonet region:

- Estimates of cloud base updraft and downdraft mass fluxes retrieved from the surface divergence field.

- Estimates of rain evaporation retrieved from cold pool pressure perturbations.

- Cold pool properties (occurrence, size, depth).

- Spatial variances of potential temperature, water vapor, moist static energy, and wind variance, at the surface.
- Precipitation rate and area fraction.

2.2 Actual accomplishments

We thoroughly investigated the first two hypotheses:

1. Updraft and downdraft cumulus mass fluxes can be retrieved or estimated from surface mesonet observations of wind velocity combined with gridded precipitation rate.
2. Cold pool properties can be retrieved or estimated from surface mesonet observations of temperature, water vapor, and pressure.

The actual data products that we produced were based on 15 full years (not 13 warm seasons) of Oklahoma Mesonet data. They include the following hourly time series for the Oklahoma Mesonet region:

- Statistics of the surface divergence field from which estimates of near-cloud-base updraft and downdraft mass fluxes can be made.
- Spatial variances of potential temperature, water vapor, moist static energy, and wind variance, at the surface.
- Precipitation rate and area fraction.

The data products that we produced also include complete catalogs of:

- Frontal passage properties (time and location, temperature drop and pressure rise).
- Cold pool properties (time and location, size, duration, temperature drop and pressure rise).

3 Project Activities

3.1 Retrieving updraft and downdraft cumulus mass fluxes from mesonet observations

The Oklahoma Mesonet surface wind data and the Arkansas Basin River Forecast Center (ABRFC) gridded precipitation data from May to August, 1997, were used to demonstrate and evaluate a new method for retrieving the area-averaged cloud-base updraft and downdraft mass fluxes from statistics of the surface divergence field (Sun and Krueger 2012). Because there are no direct observations of cloud-base mass fluxes, the gridded precipitation data were used as a proxy. These observational results indicate that it is possible to retrieve cloud-base mass fluxes from statistics of the mesoscale surface divergence field.

We also performed an OSSE (observing system simulation experiment) based on two CRM simulations to examine the performance of the cloud-base mass flux retrieval method (Sun and Krueger 2012). The results from a 54-hour 3D simulation of a maritime tropical convective system support estimating updraft and downdraft cloud-base mass fluxes using statistics of the mesoscale surface divergence field. However there is a slight time lag in the estimated cloud-base mass fluxes relative to the actual fluxes in the simulations. The results from the 29-day 2D ARM SGP simulation of convective systems observed during the summer 1997 SCM IOP (Xu et al. 2002) also suggest that it is possible to estimate updraft and downdraft near-cloud-base mass fluxes using

Table 1: Seasonal correlations of M_u^+ and M_d^+ with mesonet precipitation for 1997-2011.

Average Correlation	Spring	Summer	Fall	Winter
M_u^+, Precip	0.50	0.59	0.45	0.31
M_d^+, Precip	0.55	0.64	0.44	0.24

statistics of the mesoscale surface divergence field. However, the peak values of the mass fluxes were not well estimated.

We also investigated whether fractional area or vertical velocity predominately determines the cloud-base mass fluxes. In the maritime tropical convective system simulation, the variations in cloud-base mass fluxes were mainly due to variations in fractional area. However, in the ARM SGP simulation, neither the vertical velocity nor the fractional area was the dominant factor in determining the cloud-base mass flux variations, which agrees with what we inferred from the Oklahoma Mesonet and gridded precipitation data.

Finally, we used the CRM simulations to compare our original cloud-base mass flux retrieval method (which relies on surface divergence statistics), with an alternative method that uses the surface precipitation instead. Generally, the precipitation method performs slightly better than the surface divergence method in both simulations. When multiple regression of the surface divergence and precipitation is used, the cloud-base mass fluxes are slightly better estimated than with either surface divergence or precipitation alone.

Later in our project, we extended the four-month, May to August 1997, analysis period described above to the 15-year, 1997-2011, period (Lesage 2013). The 15-year analysis period allowed us to obtain robust statistics for the surface divergence.

Using 10-m wind vectors, as well as the methods described in Dubois and Spencer (2005), the divergence for each mesonet triangle for every 5-minute interval was calculated. (Delauney triangulation was used to create mesonet triangles with a station at each vertex.) Sun and Krueger (2012) and Krueger and Lesage (2009) showed that certain statistics of the surface divergence field are well-correlated with precipitating cumulus updraft and downdraft near-cloud-base mass fluxes. These statistics include M_u, the mesonet average convergence in mesonet station triangles with convergence, and M_d, the mesonet average divergence in mesonet station triangles with divergence. M_u^+ and M_d^+ are the similar to these except that only triangles with convergence or divergence $> 10^{-4}$ s^{-1} are included. Sun and Krueger (2012) and Krueger and Lesage (2009) found that M_u and M_u^+ are correlated with near-cloud-base updraft mass fluxes, while M_d and M_d^+ are correlated with near-cloud-base downdraft mass fluxes. The composite annual cycle for the "downdraft mass fluxes" (M_d) exhibits slightly stronger values on average in the spring and summer than in the fall and winter (Fig. 1).

Correlations were calculated for several combinations of divergence statistics and precipitation from the Oklahoma Mesonet. The most notable result was that M_u^+ and M_d^+ are correlated most strongly with precipitation in the summer, and least in the winter (Table 1).

"Dry" and "wet" days were identified for the Oklahoma Mesonet. DRy days haD no precipitation and wet days had at least 1 mm of precipitation on average over the Mesonet. Average strong convergence values for the Oklahoma mesonet by season and wet/dry days are shown in Fig. 2. Spring and summer wet days had the highest average M_u^+. In every season, M_u^+ was larger on average for wet days than for dry days: about twice as large in spring and summer, and about 10 percent larger in winter.

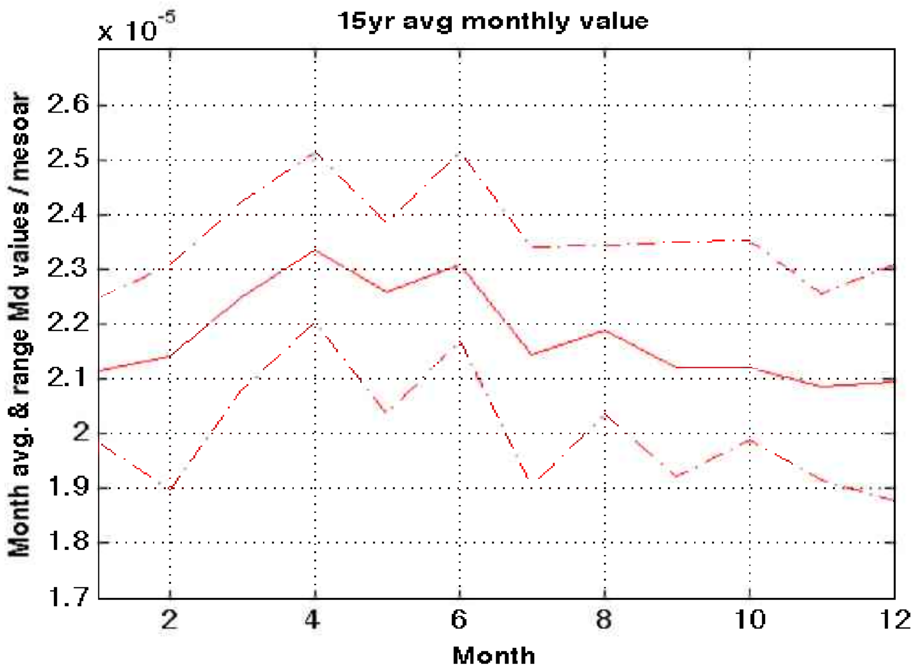

Figure 1: Average monthly M_d values and their ranges for the Oklahoma Mesonet for 1997-2011.

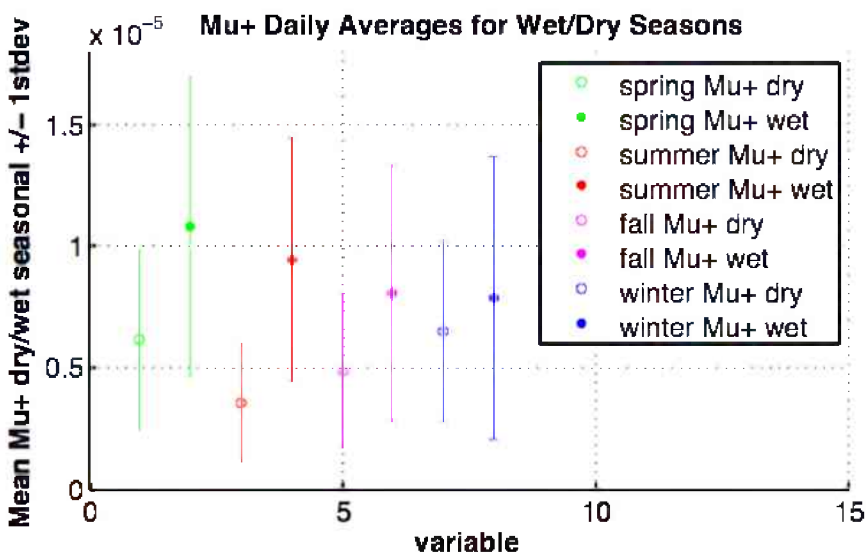

Figure 2: Seasonal average M_u^+ values for the Oklahoma Mesonet over the 1997-2011 period for wet and dry days.

3.2 Retrieving convective cold pool properties from mesonet observations

We also retrieved information about convective cold pool properties from the 15 years of 5-minute Oklahoma Mesonet data and hourly Arkansas Basin River Forecast Center (ABRFC) gridded precipitation data.

3.2.1 Mesoanalyis procedures

We implemented and tested a set of mesoanalyis procedures used by Adams-Selin and Johnson (2010). The effect of station elevation was removed from the pressure dataset using the method of Loehrer and Johnson (1995). The station pressure was adjusted to 356.5 m, the mean height of the mesonet stations. Diurnal and semi-diurnal tidal oscillations were removed from the station pressure data using the procedure described in Johnson and Hamilton (1988). As the focus of our study was on mesoscale features, synoptic-scale effects were removed by applying a Lanczos high-pass Fourier filter (Duchon 1979) to the data. Low-frequency oscillations with periods greater than 82.4 h, or twice the length of a pendulum day for the average latitude in Oklahoma, were considered synoptic-scale phenomena that were irrelevant for this study and thus were removed by this filter. Adams-Selin and Johnson analysed four years (2002-2005) of Oklahoma Mesonet data using this set of procedures, and kindly made their processed station data available to us to check the results of our own analyses.

3.2.2 Estimating rain evaporation from cold pool pressure perturbations

We developed a method to estimate rain evaporation in convective systems from the cold pool surface pressure perturbations obtained from the mesoanalysis procedure just described (Krueger and Lesage 2010). In the 1950s, Fujita identified meso-highs in his mesoanalyses and linked them to cold pools produced by rain evaporation (Fujita 1959). We are extending Fujitas (1959) method for estimating rain evaporation from the hydrostatic surface pressure anomaly.

In order to test Fujitas (1959) method, we obtained a 3D numerical model based on the unified system of equations (Arakawa and Konor 2009). This system unifies the nonhydrostatic anelastic system and the quasi-hydrostatic compressible system for use in very-large-domain cloud-resolving models. The system is fully compressible for quasi-hydrostatic motion and anelastic for purely nonhydrostatic motion. In this way, the system can cover a wide range of horizontal scales from turbulence to planetary waves. Such a model is ideally suited for simulating surface pressure perturbations due to rain evaporation in msesoscale convective systems.

3.2.3 Front and cold pool detection and properties

An analysis of 15 years of Oklahoma Mesonet near-surface data, covering the 1997-2011 period, has been performed in order to detect fronts and cold pools and document their properties (Lesage and Krueger 2011a,b, 2012, Lesage 2013, Lesage and Krueger 2014a). The 104 Mesonet stations present in 1997 were used in this study. Each year of a station's data were included if at least 95% of the year's 5-minute observations had the key variables (1.5-m temperature, surface pressure, 10-m wind speed and direction, and relative humidity) observed. This criterion resulted in between 99 and 104 stations being used for each of the 15 years.

Methods were developed to identify the locations of both frontal passages and cold pools using these near-surface observations. Identifying frontal passages starts with developing the cold pool score (CPS). This unitless measure combines temperature falls and pressure rises over 30-minute periods computed every 5-minute interval for each of the Mesonet stations. A pressure rise of 1 mb is considered equivalent to 1 K of temperature drop with each contributing 1 to the CPS. Pressure and temperature are utilized due to their usefulness in defining fronts in a study by Engerer et al. (2008). Both temperature and pressure had elevation adjustments made to the average height of the Mesonet stations, as well as removal of the diurnal cycle. A front is defined to have reached a

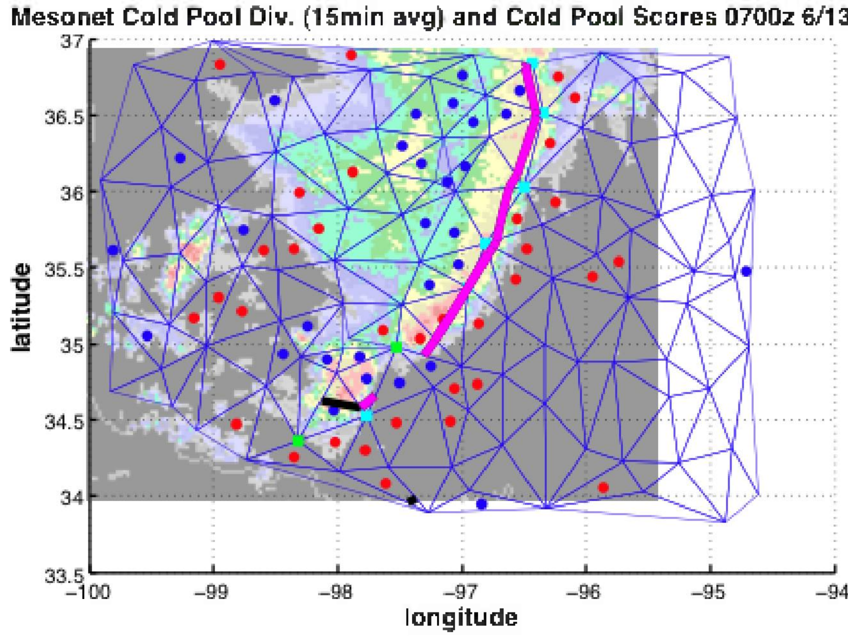

Figure 3: Front analysis for 07Z June 13, 1997. Red dots are regions of strong convergence while blue dots are regions of strong divergence. Black (magenta) lines mark frontal passages where all corners of the triangle reach cold pool scores > 3 (> 5). Green (cyan) squares are stations that currently have cold pool scores > 3 (> 5).

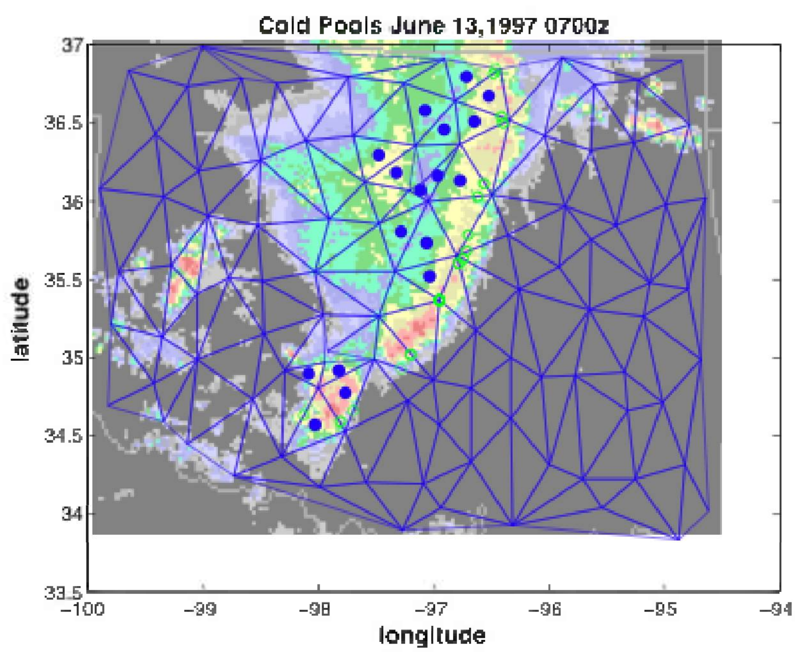

Figure 4: Cold pool analysis for 07Z June 13, 1997. Blue dots represent triangles currently in cold pools. Green open circles indicate the front location.

Mesonet station when the CPS at a station exceeds a minimum threshold and when the CPS is the highest it reaches within 3 hours in either direction. In this study, 3 and 5 are used as thresholds for fronts and strong fronts respectively. If the stations at all three corners of a Mesonet triangle meet the frontal passage threshold within a 2-hour interval, the triangle is considered to have undergone a frontal passage. Fig. 3 is an example of a frontal analysis.

A cold pool occurs for a mesonet triangle if the triangle experiences a frontal passage, and if there is strong divergence within half an hour before or an hour after the frontal passage. Strong divergence is considered to be divergence larger than 1x10^{-4} s^{-1}. The duration of the cold pool is considered to be the interval which includes the divergence maximum and extends temporally in both directions until divergence is less than half the maximum value. An example of a cold pool analysis is shown in Fig. 4.

The remainder of this section documents the key results from the study: Δp and ΔT correlations, and diurnal, seasonal, and geographic distributions of frontal passages. For each frontal passage at a station, the Δp and ΔT values were calculated based on the largest pressure increase and temperature decrease between 30 minutes before frontal passage and 2 hours after frontal passage. Statistics for this analysis are shown in Table 2. Notably, summer had the lowest changes in pressure with frontal passages and the lowest correlation between Δp and ΔT, while spring and winter had the highest correlations and pressure changes. About 2/3 of the frontal passages occurred during spring and summer.

The seasonal distribution of frontal passages across station triangles was also calculated, along with the number that included cold pools (Table 3). Three-quarters of the yearly total of cold pools occurred during spring and summer. During spring, 59% of the fronts had cold pools, while during summer, 80% did, and during winter, only 35% did. The percentages with cold pools were 6-8% greater for strong fronts.

Diurnal distributions of frontal passages were also computed for 1997-2011. The diurnal distribution of fronts varies by season. During the summer there is a distinct peak around 22 UTC (17 LST) while in other seasons, the distribution has less well-defined maxima (Fig. 5).

The geographic frequency of frontal passages across the Mesonet was computed as well. Fig. 6 shows that the annual average frontal passage frequency significantly decreases from west to east.

3.2.4 Front and cold pool case studies

By applying the methods already described to 15 years of data, tens of thousands of frontal passages were detected in the Oklahoma Mesonet. There were hundreds of events that involved a front that swept through a large portion of the Mesonet. We analyzed four such cases in detail: (1) 13 June 1997, (2) 15-16 June 2002, () 20 May 2011, and (4) 24-25 May 2011 (Lesage and Krueger 2014b).

Table 2: Δp and ΔT seasonal statistics and correlations, as well as frontal passage seasonal frequency for stations. All stats are given for CPS > 3 / CPS > 5.

1997-2011	ΔT avg.	Δp avg.	$\Delta T \Delta p$ correlation	Frontal Passages at Stations
Total	-6.1K/-8.1K	+2.5K/+3.2K	-0.28/-0.33	72,571/25,313
Spring (MAM)	-5.8K/-7.6K	+2.8K/+3.6K	-0.32/-0.43	22,747/7,844
Summer (JJA)	-6.1K/-7.6K	+2.0K/+2.5K	-0.15/-0.06	23,342/9,768
Fall (SON)	-6.1K/-8.3K	+2.4K/+3.1K	-0.23/-0.17	13,440/4,283
Winter (DJF)	-6.6K/-10.2K	+2.9K/+4.4K	-0.41/-0.38	13,042/3,418

Table 3: Frontal passage and cold pool seasonal statistics. All stats are given for CPS > 3 / CPS > 5.

1997-2011	Total # Triangles in Fronts	# Fronts w/ Cold Pools	% of Fronts w/ Cold Pools
Total	74,906/26,551	44,967/18,161	60.0%/68.4%
Spring (MAM)	24,684/8,635	14,493/5,644	58.7%/65.4%
Summer (JJA)	23,706/9,362	18,859/8,170	79.6%/87.3%
Fall (SON)	13,500/4,579	6,993/2,719	51.8%/59.4%
Winter (DJF)	13,016/3,975	4,622/1,628	35.5%/41.0%

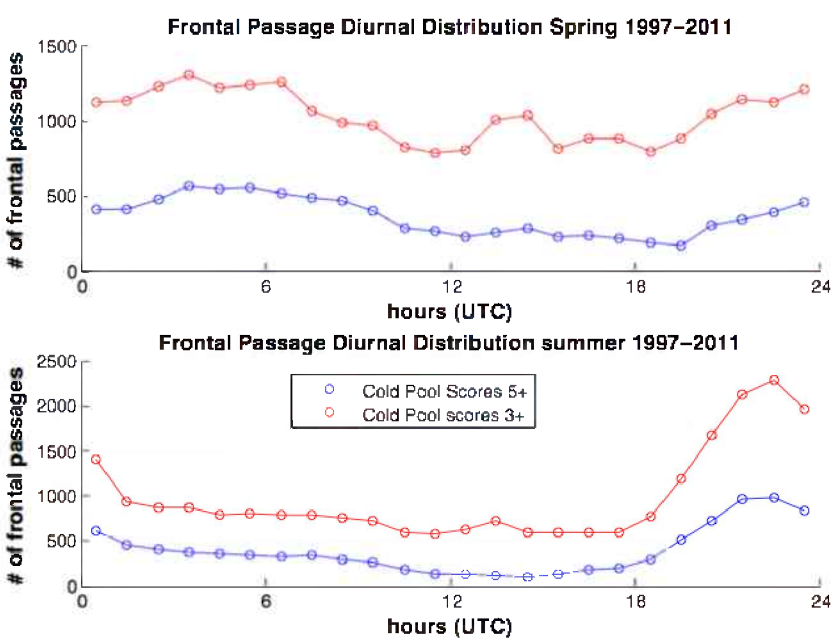

Figure 5: Diurnal distribution of frontal passages for the spring (MAM) and summer (JJA) for 1997-2011 Oklahoma Mesonet data for all cold pools and for strong cold pools.

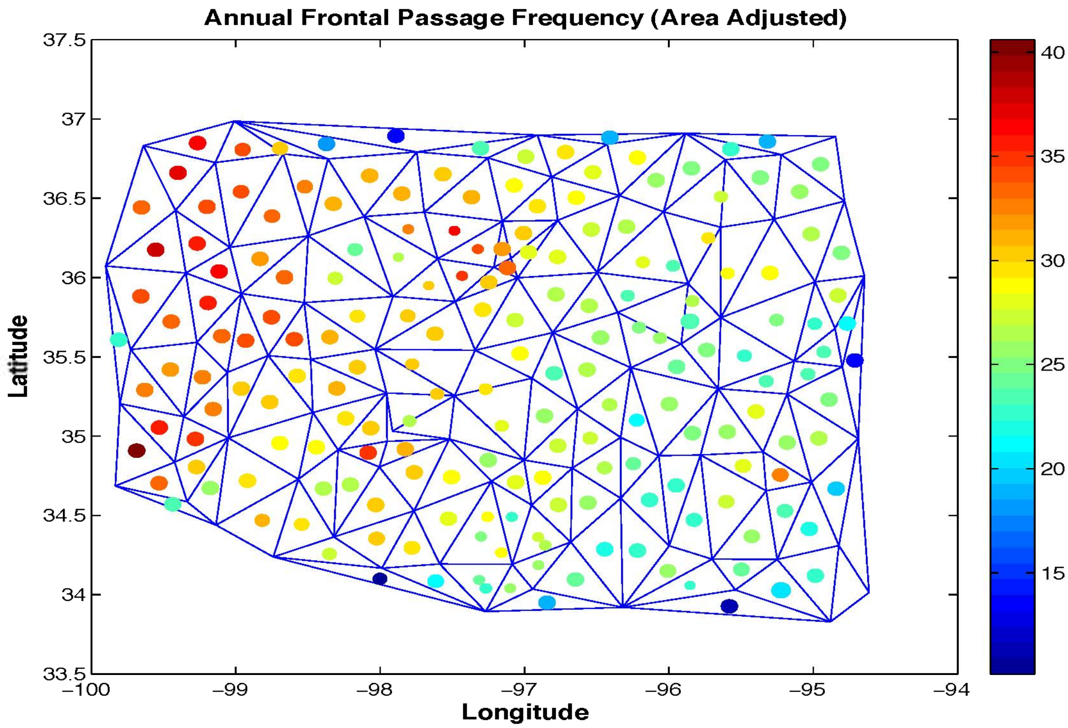

Figure 6: Frontal passage distribution for 1997-2011. Dot size represents the number of years a triangle centroid was in that location. The triangles are for the 1997 station locations.

For example, the first case involved a squall line that was initiated in southeastern Colorado and northeastern New Mexico, then entered Kansas, the Oklahoma panhandle, and Texas. The line of thunderstorms entered the Oklahoma Mesonet at roughly 0300 UTC on 13 June 1997 and was tracked for the next seven hours as it crossed the mesonet, as shown in Fig. 7. Plotting the evolution of the cold pool areas is an effective way to compare cold pool sizes and durations of the four cases, as shown in Fig. 8. We also compared the average time series (relative to the time of frontal passage) of divergence, temperature, and pressure during frontal passages for the four cases (not shown). The time series are qualitatively the same, but differ quantitatively. Using the frontal passage times at the corners of each mesonet triangle, we calculated the speed and direction of the front for each triangle (not shown). The front speeds vary from case to case, and also during each case, and are mostly between 10 and 20 m/s.

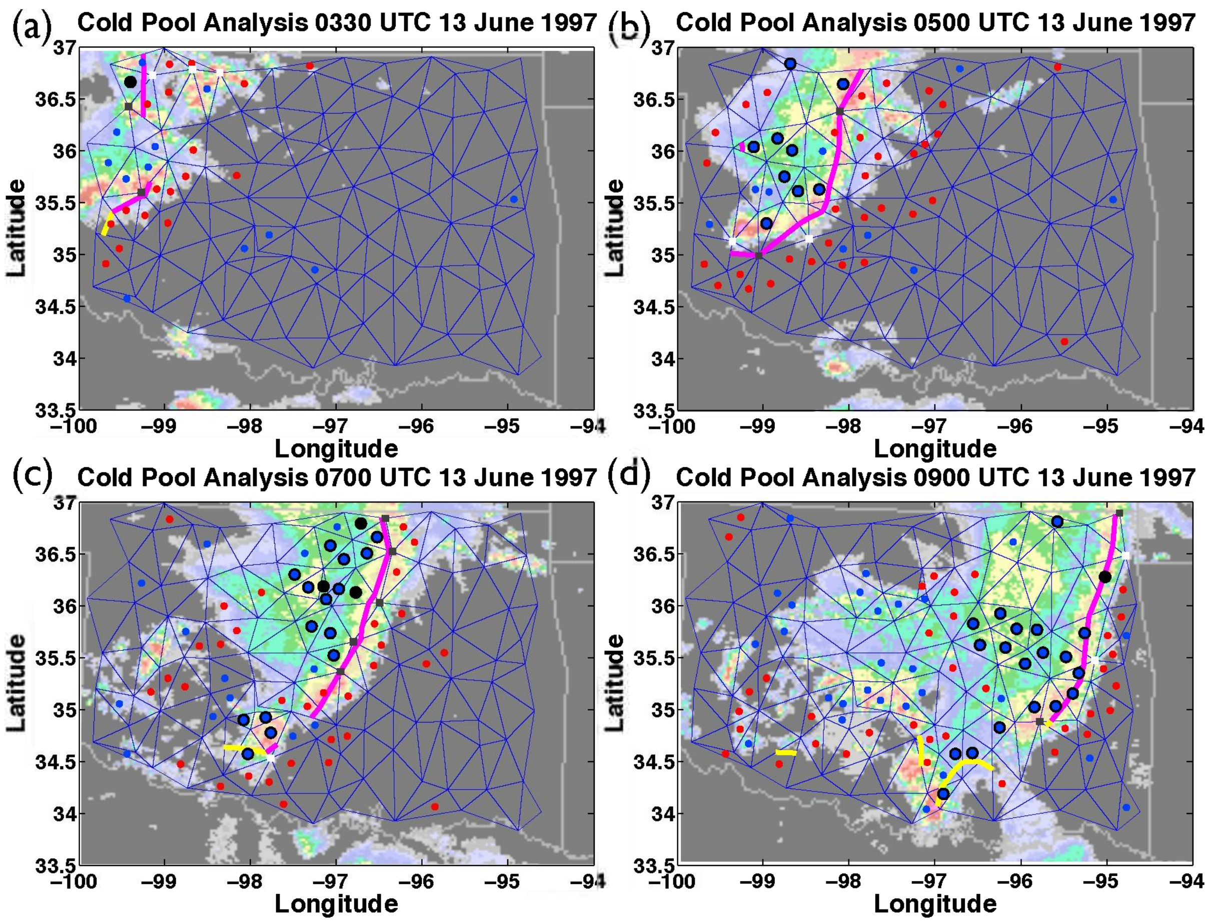

Figure 7: Front and cold pool analysis for 13 June 1997 (a) 0300 UTC, (b) 0500 UTC, (c) 0700 UTC, and (d) 0900 UTC. Red dots indicate mesonet triangles with divergence $< -10^{-4}$ s^{-1} while blue dots indicate those with divergence $> 10^{-4}$ s^{-1}. Yellow lines are fronts with $3 \leq$ FrontScore < 5 while magenta lines are fronts with FrontScore > 5. White squares are stations with $3 \leq$ FrontScore < 5 while gray squares designate stations with FrontScore > 5. Black dots indicate mesonet triangles designated as cold pools. Color shading indicates radar reflectivity. Radar images are from the UCAR image archive, NEXLAB - College of DuPage.

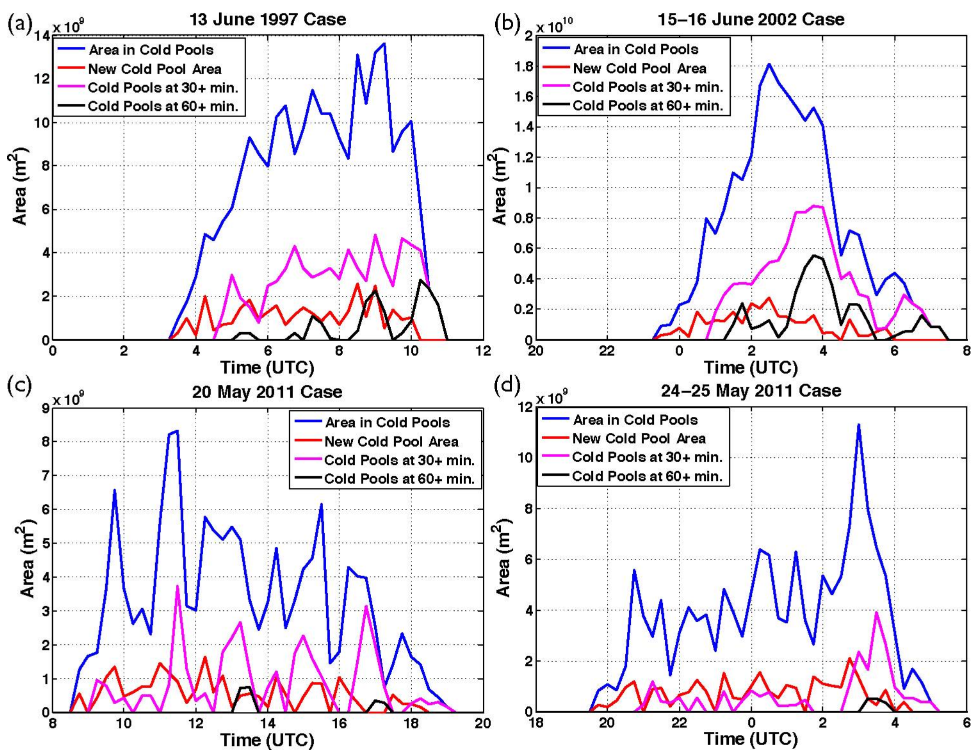

Figure 8: Cold pool areas for the four case studies. Cold pool areas are shown as 15-minute averages for total area in cold pools (blue), area that becomes part of a cold pool in each 15-minute time interval (red), area residing in a cold pool for at least 30 minutes (magenta), and area residing in a cold pool for at least 60 minutes (black).

4 References

Adams-Selin, R. D. and R. H. Johnson, 2010: Mesoscale surface pressure and temperature features associated with bow echos. *Mon. Wea. Rev.*, **138**, 212–227, doi:10.1175/2009MWR2892.1.

Arakawa, A. and C. S. Konor, 2009: Unification of the anelastic and quasi-hydrostatic systems of equations. *Mon. Wea. Rev.*, **137**, 710–726.

Dubois, J. A. and P. L. Spencer, 2005: Computing divergence from a surface network: Comparison of the triangle and pentagon methods. *Wea. Forecasting*, **20**, 596–608.

Duchon, C. E., 1979: Lanczos filtering in one and two dimensions. *J. Appl. Meteor.*, **18**, 1016–1022.

Engerer, N. A., D. Stensrud, and C. Coniglio, 2008: surface characterisitcs of observed cold pools. *Mon. Wea. Rev.*, **136**, 4838–4849, doi:10.1175/2008MWR2528.1.

Fujita, T., 1959: Precipitation and cold air production in mesoscale thunderstorm systems. *J. Meteor.*, **16**, 454–466.

Johnson, R. H. and P. J. Hamilton, 1988: The relationship of surface pressure features to the precipitation and airflow structure of an intense midlatitude squall line. *Mon. Wea. Rev.*, **116**, 1444–1473.

Krueger, S. K. and A. T. Lesage, 2009: Mesoanalysis and numerical modeling of the interactions of precipitating convection and the boundary layer. *Atmospheric Radiation Measurement (ARM) Science Team Meeting.*, http://www.arm.gov/publications/proceedings/conf19/display?id=Njg4.

Krueger, S. K. and A. T. Lesage, 2010: Estimating rain evaporation in convective systems from cold pool surface pressure perturbations. *1st Atmospheric System Research (ASR) Science Team Meeting.*, Bethesda, Maryland, http://asr.science.energy.gov/meetings/stm/posters/view?id=249.

Lesage, A. T., 2013: Frontal passage and cold pool detection using Oklahoma Mesonet observations. M.S. thesis, Dept. of Atmospheric Sciences, University of Utah, 73 pp.

Lesage, A. T. and S. K. Krueger, 2011a: Cold pool properties from Oklahoma Mesonet data. *2nd Atmospheric System Research (ASR) Science Team Meeting.*, San Antonio, Texas, http://asr.science.energy.gov/meetings/stm/posters/view?id=406.

Lesage, A. T. and S. K. Krueger, 2011b: Cold pool properties from Oklahoma Mesonet data. *14th Conference on Mesoscale Processes.*, Los Angeles, California, Amer. Meteor. Soc., http://ams.confex.com/ams/14Meso15ARAM/webprogram/Paper191270.html.

Lesage, A. T. and S. K. Krueger, 2012: Analysis of convectively generated cold pools and fronts from mesonet data. *3rd Atmospheric System Research (ASR) Science Team Meeting.*, Arlington, Virginia, http://asr.science.energy.gov/meetings/stm/posters/view?id=698.

Lesage, A. T. and S. K. Krueger, 2014a: Fronts and convective cold pools in the Oklahoma Mesonet. Part I: 15-year climatology. *Mon. Wea. Rev.*, submitted.

Lesage, A. T. and S. K. Krueger, 2014b: Fronts and convective cold pools in the Oklahoma Mesonet. Part II: Case studies. *Mon. Wea. Rev.*, submitted.

Loehrer, S. M. and R. H. Johnson, 1995: Surface pressure and precipitation life cycle characteristics of PRE-STORM mesoscale convective systems. *Mon. Wea. Rev.*, **123**, 600–621.

Sun, R. and S. K. Krueger, 2012: Mesoanalysis of the interactions of precipitating convection and the boundary layer. *J. Adv. Model. Earth Syst.*, **4**, M04 004, doi:10.1029/2011MS000096.

Xu, K.-M., et al., 2002: An intercomparison of cloud-resolving models with the Atmospheric Radiation Measurement summer 1997 Intensive Observation Period data. *Quart. J. Roy. Meteor. Soc.*, **128**, 593–624.

5 Publications

Refereed Publications

Giangrande, S. E., S. Collis, J. Straka, A. Protat, C. Williams, and S. Krueger, 2013: A summary of convective-core vertical velocity properties using ARM UHF wind profilers in Oklahoma. *J. Appl. Meteor. Climatol.,* **52,** 2278–2295. `http://dx.doi.org/10.1175/JAMC-D-12-0185.1`

Lesage, A. T. and S. K. Krueger, 2014: Fronts and Convective Cold Pools in the Oklahoma Mesonet. Part I: 15-Year Climatology. (Submitted to *Mon. Wea. Rev.*)

Lesage, A. T. and S. K. Krueger, 2014: Fronts and Convective Cold Pools in the Oklahoma Mesonet. Part II: Case Studies. (Submitted to *Mon. Wea. Rev.*)

Lu, C., Y. Liu, S. Niu, S. K. Krueger, and T. Wagner, 2013: Exploring parameterization for turbulent entrainment-mixing processes in clouds. *J. Geophys. Res. Atmos.,* **118,** 185–194. `http://dx.doi.org/10.1029/2012JD018464`

Sun, R., and S. K. Krueger, 2012: Mesoanalysis of the interactions of precipitating convection and the boundary layer. *J. Adv. Model. Earth Syst.,* **4,** M04004, `doi:10.1029/2011MS000096`.

Wagner,T. J. , D. D. Turner, L. K. Berg, and S. K. Krueger, 2013: Ground-based remote retrievals of cumulus entrainment rates. *J. Atmos. Ocean. Tech.,* **30,** 1460–1471. `http://dx.doi.org/10.1175/JTECH-D-12-00187.1`

Dissertations and Theses

Lesage, Andrew T., 2013: Frontal Passage and Cold Pool Detection using Oklahoma Mesonet Observations. M. S. Thesis, University of Utah, Salt Lake City, 73 pp.

Other Publications

Krueger, S., and R. Sun, 2009: Mesoanalysis and Numerical Modeling of the Interactions of Precipitating Convection and the Boundary Layer. *Nineteenth Atmospheric Radiation Measurement (ARM) Science Team Meeting,* Louisville, KY, Mar 30-Apr 4, 2009. `http://www.arm.gov/publications/proceedings/conf19/display?id=Njg4`

Krueger, S. K. and A. T. Lesage, 2010: Estimating rain evaporation in convective systems from cold pool surface pressure perturbations. *1st Atmospheric System Research (ASR) Science Team Meeting*, Bethesda, Maryland, `http://asr.science.energy.gov/meetings/stm/posters/view?id=249`

Lesage, A. T. and S. K. Krueger, 2011a: Cold pool properties from Oklahoma Mesonet data. *2nd Atmospheric System Research (ASR) Science Team Meeting*, San Antonio, Texas, `http://asr.science.energy.gov/meetings/stm/posters/view?id=406`

Lesage, A. T. and S. K. Krueger, 2011b: Cold pool properties from Oklahoma Mesonet data. *14th Conference on Mesoscale Processes*, Los Angeles, California, Amer. Meteor. Soc., `http://ams.confex.com/ams/14Meso15ARAM/webprogram/Paper191270.html`

Lesage, A. T. and S. K. Krueger, 2012: Analysis of convectively generated cold pools and fronts from mesonet data. *3rd Atmospheric System Research (ASR) Science Team Meeting*, Arlington, Virginia, `http://asr.science.energy.gov/meetings/stm/posters/view?id=698`

Sun, R., S. K. Krueger, Y. Li, and M. A. Zulauf, 2008: Mesoanalysis of the Interactions of Precipitating Convection and the Boundary Layer. *Eighteenth Atmospheric Radiation Measurement (ARM) Science Team Meeting,* Norfolk, VA. http://www.arm.gov/publications/proceedings/conf18/poster/P00159.pdf

Sun, R., and S. K. Krueger, 2008: Mesoanalysis of the Interactions of Precipitating Convection and the Boundary Layer. *15th Conference on Clouds and Precipitation,* Cancun, Mexico, July 2008.